PHYSICAL REVIEW A **86**, 040501(R) (2012)

Shifts due to distant neighboring resonances for laser measurements of $2\,^3S_1$-to-$2\,^3P_J$ transitions of helium

A. Marsman, M. Horbatsch,* and E. A. Hessels
Department of Physics and Astronomy, York University, Toronto, Ontario M3J 1P3, Canada
(Received 25 August 2012; published 1 October 2012)

Quantum-mechanical interference between transitions from the metastable $2\,^3S_1 m_J = 0$ state to $2\,^3P_1 m_J = \pm 1$ and to $2\,^3P_2 m_J = \pm 1$ is shown to cause shifts in these resonances, despite the fact that the resonances are separated by more than 1000 natural widths. The $2\,^3P_1$-to-$2\,^3P_2$ fine-structure interval can be determined from the difference of these laser transitions, and a comparison between experiment and theory for this interval allows for precise tests of the quantum-electrodynamic (QED) theory used to calculate the interval. The shifts described here are large enough to be important for this test of QED and therefore to affect the continuing program of determining the fine-structure constant from comparison between accurate experimental measurements and theoretical calculations of the helium $2\,^3P$ energy intervals.

DOI: 10.1103/PhysRevA.86.040501 PACS number(s): 32.70.Jz, 32.80.−t

Analytic calculations in simple three- and four-level systems indicate that distant neighboring resonances can cause shifts [1] in observed resonances for atoms experiencing a field of constant amplitude and frequency. Here, distant neighboring resonance refers to the case in which the nearest resonance is separated by many natural widths from the main resonance being considered. These simplified calculations set a scale for the expected shifts, but are not directly applicable to more complicated (and more realistic) situations, in which a larger set of states allows for additional atomic processes and time-dependent amplitudes are present. In a recent work [2], the analysis was extended to a multilevel atomic system and shifts for the atomic helium $2\,^3P_1$-to-$2\,^3P_2$ and $2\,^3P_1$-to-$2\,^3P_0$ microwave transitions were calculated. The shifts were calculated for both experiments which use a single pulse of microwaves and which use the Ramsey technique of separated oscillatory fields. The shifts found in that work were too small to be of concern for currently completed microwave measurements [3,4], but will be of importance for improved measurements that are presently being performed.

Here we calculate the shifts for laser transitions from the metastable $2\,^3S_1 m_J = 0$ state to $2\,^3P_1 m_J = \pm 1$ and to $2\,^3P_2 m_J = \pm 1$ (see Fig. 1). The $2\,^3P_1$-to-$2\,^3P_2$ fine-structure interval can be determined from the difference between the resonant frequencies for these laser transitions. A comparison between experiment and theory for this $2\,^3P$ fine-structure interval provides an important test of quantum-electrodynamic (QED) theory.

A comparison between theory and experiment for the larger $2\,^3P_2$-to-$2\,^3P_0$ (or $2\,^3P_1$-to-$2\,^3P_0$) interval of Fig. 1 allows for a precise determination of α. A similar comparison of the smaller $2\,^3P_2$-to-$2\,^3P_1$ interval (at a similar absolute accuracy) is, because of the smaller interval size, not a good candidate for determining α, but serves instead to provide an independent test of the theory necessary for the α determination. This program for determining α has been ongoing for almost 50 years [5], with extensive theoretical [6–12] and experimental [3,4,13–18] contributions, and a determination of α to better than a part per billion may soon be possible.

The shifts found in this work lead to a correction to a measurement [15] of the $2\,^3P_1$-to-$2\,^3P_2$ interval that is larger than the experimental uncertainty and is significant for comparisons between experimental results and theory for this interval and for the ongoing program of determining α from the helium fine-structure intervals.

For the present work, we follow the experimental technique used in Ref. [15] and assume that the metastable $2\,^3S_1 m_J = 0$ state (denoted $|1\rangle$ in Fig. 1) is initially populated (i.e., in terms of the density matrix, $\rho_{11} = 1$) and a 1083 nm circularly polarized laser with either σ_- or σ_+ polarization drives $2\,^3S$-to-$2\,^3P$ transitions. For $\sigma_\pm$ polarization, the $2\,^3S_1 m_J = 0$-to-$2\,^3P_1 m_J = \pm 1$ transition (the solid arrows from $|1\rangle$ to $|2\rangle$ in Fig. 1) and the $2\,^3S_1 m_J = 0$-to-$2\,^3P_2 m_J = \pm 1$ transition (the dashed arrows from $|1\rangle$ to $|3\rangle$) can be driven, and, in each case (that is, for each of the two circular polarizations), the energy spacing between the $2\,^3P_1$ and $2\,^3P_2$ levels can be determined from the differences between the observed resonant frequencies.

When the laser is nearly resonant with the $|1\rangle \rightarrow |2\rangle$ transition, there are shifts (that are significant for a 1 kHz accuracy measurement of this 1.63 MHz natural-width resonance) due to interference with the distant $|1\rangle \rightarrow |3\rangle$ transition, despite the fact that the transitions are separated by 1400 natural widths. Similarly, when the laser field that is nearly resonant with the $|1\rangle \rightarrow |3\rangle$ transition, there are shifts due to the distant $|1\rangle \rightarrow |2\rangle$ transition. The purpose of this work is to calculate these interference shifts.

Figure 2 shows the timing diagram being considered here for a metastable atom passing through a laser beam. The atom is assumed to start in $|1\rangle$ at a time t_i before it enters the laser beam. The time profile of the laser intensity is Gaussian, with $1/e$ width T_L, which is determined by the speed of the atom and the waist of the laser beam, and with the maximum intensity I_0, which is determined by the power of the laser beam, the laser beam waist, and the atom's trajectory through the laser beam. The atoms that end up in $|0\rangle$ are detected at a later time t_f after the atom has traversed the laser beam and after sufficient time has passed for the $2\,^3P$ excited-state atoms to radiatively decay back to the $2\,^3S$ metastable states.

In the electric-dipole approximation, $U(t) = e\vec{r} \cdot \vec{E}(t)$ couples $|1\rangle$ to both $|2\rangle$ and $|3\rangle$. For $\sigma_\pm$ polarization,

*marko@yorku.ca

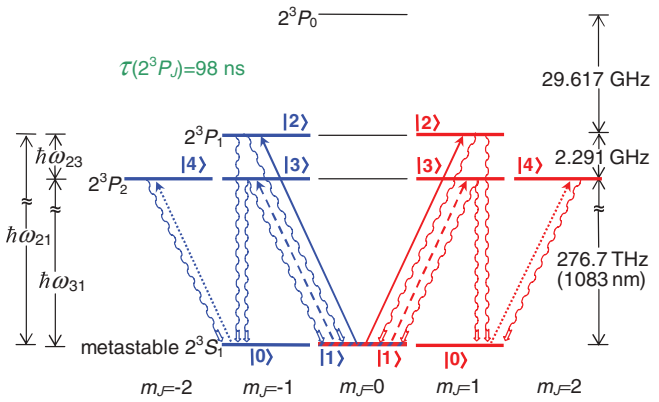

FIG. 1. (Color online) The $n = 2$ triplet energy levels of helium. Population starts in $|1\rangle$ and interacts with a circularly polarized laser field. For σ_-, the states on the left ($|0\rangle$ to $|4\rangle$ in blue) can be populated. Quantum-mechanical interference between the $|1\rangle \rightarrow |2\rangle$ (solid arrow) and $|1\rangle \rightarrow |3\rangle$ (dashed arrow) transitions causes shifts in the measured resonances. Similar transitions with positive m_J result from σ_+, as shown at the right in red. The cycling transition (dotted arrow) and the allowed radiative decay paths are also shown.

$\vec{E}(t) = E_0 g(t)[\hat{x}\cos(\omega t + \phi) - \hat{y}\cos(\omega t + \phi \pm \pi/2)]/\sqrt{2}$, with $g(t) = \exp[-2(t - t_L)^2/{T_L}^2]$. We use the rotating-wave approximation, in which the nonresonant $\exp(-i\omega t - i\theta)$ part of $\cos(\omega t + \theta)$ is ignored. As shown in Fig. 1, $|2\rangle$ and $|3\rangle$ both have rates for radiative decay down to $|1\rangle$ and $|0\rangle$. $U(t)$ also couples $|0\rangle$ to the $2\,^3P_2 m_J = 2$ state ($|4\rangle$ in Fig. 1). However, since $|4\rangle$ always decays back to $|0\rangle$, any atom that makes it into $|0\rangle$ can only cycle between $|0\rangle$ and $|4\rangle$ and, by time t_f (after sufficient time for radiative decay), will necessarily be found in $|0\rangle$.

The density matrix equations for determining the population in $|1\rangle$, $|2\rangle$, and $|3\rangle$ for a laser frequency $\omega = 2\pi f$ that is nearly in resonance with the $|1\rangle \rightarrow |2\rangle$ transition in Fig. 1, are [1,19]

$$\dot{\rho}_{11} = \frac{i\Omega_2}{2}\rho_{12} - \frac{i\Omega_2^*}{2}\rho_{21} + \gamma_{2\rightarrow1}\rho_{22} + \frac{i\Omega_3}{2}\rho_{13} - \frac{i\Omega_3^*}{2}\rho_{31} + \gamma_{23\rightarrow1}(\rho_{23} + \rho_{32}) + \gamma_{3\rightarrow1}\rho_{33}, \quad (1a)$$

$$\dot{\rho}_{12} = \frac{i\Omega_2^*}{2}(\rho_{11} - \rho_{22}) - \left(\frac{\gamma_2}{2} + i\Delta_2\right)\rho_{12} - \frac{\gamma_{23}}{2}\rho_{13} - \frac{i\Omega_3^*}{2}\rho_{32}, \quad (1b)$$

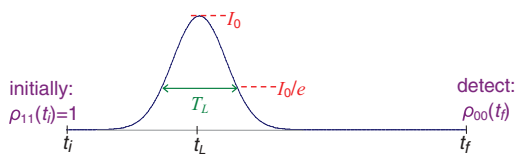

FIG. 2. (Color online) Timing for the atom traveling through a Gaussian laser beam with peak intensity I_0. The atom starts in $|1\rangle$ of Fig. 1 at a time t_i before the atom enters the laser beam, and the final population of $|0\rangle$ is determined at a time t_f after it has left the laser beam, and after the $2\,^3P$ atoms have had time to decay back to the $2\,^3S$ states.

$$\dot{\rho}_{22} = \frac{i\Omega_2^*}{2}\rho_{21} - \frac{i\Omega_2}{2}\rho_{12} - \gamma_2\rho_{22} - \frac{\gamma_{23}}{2}(\rho_{23} + \rho_{32}), \quad (1c)$$

$$\dot{\rho}_{13} = \frac{i\Omega_3^*}{2}(\rho_{11} - \rho_{33}) - \frac{\gamma_{23}}{2}\rho_{12} - \frac{i\Omega_2^*}{2}\rho_{23} - \left(\frac{\gamma_3}{2} + i(\Delta_2 + \omega_{23})\right)\rho_{13}, \quad (1d)$$

$$\dot{\rho}_{23} = \frac{i\Omega_3^*}{2}\rho_{21} - \frac{\gamma_{23}}{2}(\rho_{22} + \rho_{33}) - \frac{i\Omega_2}{2}\rho_{13} - \left(\frac{\gamma_2 + \gamma_3}{2} + i\omega_{23}\right)\rho_{23}, \quad (1e)$$

$$\dot{\rho}_{33} = \frac{i\Omega_3^*}{2}\rho_{31} - \frac{i\Omega_3}{2}\rho_{13} - \gamma_3\rho_{33} - \frac{\gamma_{23}}{2}(\rho_{23} + \rho_{32}), \quad (1f)$$

where $\Omega_k = \Omega_k(t) = \frac{1}{\sqrt{2}}eE_0 g(t)e^{i\phi}\langle 1|x \mp iy|k\rangle/\hbar$ are time-dependent Rabi frequencies, Ω_k^* are their complex conjugates, $\Delta_2 = \omega - \omega_{21}$ is the amount by which the laser is detuned from the $|1\rangle \rightarrow |2\rangle$ transition, and $\hbar\omega_{21}$ and $\hbar\omega_{23}$ are the energy differences shown in Fig. 1. From the ratio of the electric-dipole matrix elements, Ω_2 and Ω_3 are related by $\Omega_2 = \pm\Omega_3$ (for $\sigma_\pm$ polarization). The radiative decay rates γ_2, γ_3, and γ_{23} can be written in terms of the partial decay rates $\gamma_2 = \gamma_{2\rightarrow1} + \gamma_{2\rightarrow0}$, $\gamma_3 = \gamma_{3\rightarrow1} + \gamma_{3\rightarrow0}$, and $\gamma_{23} = \gamma_{23\rightarrow1} + \gamma_{23\rightarrow0}$ where, in the electric-dipole approximation,

$$\gamma_{i\rightarrow j} = \frac{4e^2|\omega_{ji}|^3}{3\hbar c^3}\langle i|\vec{r}\,|j\rangle\cdot\langle j|\vec{r}\,|i\rangle, \qquad \gamma_{23\rightarrow j} = \frac{4e^2|\omega_{j2}|^3}{3\hbar c^3}\langle 2|\vec{r}\,|j\rangle\cdot\langle j|\vec{r}\,|3\rangle. \quad (2)$$

Since $\omega_{12} \gg \omega_{23}$ (as shown in Fig. 1), $\gamma_2 = \gamma_3$, and both are equal to $\gamma = 1/\tau$, where $\tau = 97.9$ ns. From the electric dipole matrix elements, the partial rates are $\gamma_{2\rightarrow1} = \gamma_{3\rightarrow1} = \gamma_{2\rightarrow0} = \gamma_{3\rightarrow0} = \gamma/2, \gamma_{23\rightarrow1} = \pm\gamma/2$, and $\gamma_{23\rightarrow0} = \mp\gamma/2$ (for $\sigma_\pm$ polarization). The nonzero $\gamma_{23\rightarrow1}$ term in Eq. (1) results directly from quantum mechanical interference of the radiative decay and leads to the shifts discussed in this work. The opposite signs of $\gamma_{23\rightarrow0}$ and $\gamma_{23\rightarrow1}$ lead to $\gamma_{23} = 0$.

Since the population starts in $|1\rangle$ and the $|1\rangle \rightarrow |3\rangle$ transition is far out of resonance, very little population is excited to $|3\rangle$. As in Ref. [1], we introduce a small ordering parameter η and, in terms of this parameter, $\rho_{33} \lesssim \eta^2$. For this to occur, it is necessary that $\gamma_{2\rightarrow1}$, $\gamma_{2\rightarrow0}$, $\gamma_{3\rightarrow1}$, $\gamma_{3\rightarrow0}$, $|\gamma_{23\rightarrow1}|$, $|\gamma_{23\rightarrow0}|$, $|\Delta_2|$, $|\Omega_2|$, $|\Omega_3|$, and $2\pi/T$ all be smaller (by one order of η) than ω_{23}. Here, $\gamma_{2\rightarrow1} = \gamma_{2\rightarrow0} = \gamma_{3\rightarrow1} = \gamma_{3\rightarrow0} = |\gamma_{23\rightarrow1}| = |\gamma_{23\rightarrow0}| = \gamma/2 = 5.11$ MHz, and $|\Omega_2| = |\Omega_3|$ and $2\pi/T$ must be $\lesssim\gamma$ to avoid substantial broadening of the observed resonance. Furthermore, as the laser frequency is tuned across the resonance, $|\Delta_2|$ also takes on values $\lesssim$ the width of the resonance (i.e., also of order γ). All of these values are a factor of >1000 less than $\omega_{23} = 2\pi(2291$ MHz), which justifies the use of the ordering parameter η. The density matrix elements ρ_{13}, ρ_{31}, ρ_{23}, and ρ_{32} will also be an order of η smaller than the dominant elements: ρ_{11}, ρ_{12}, ρ_{21}, and ρ_{22}.

Taking linear combinations of Eqs. 1(a) through 1(e) (and their complex conjugates) allows one to eliminate (to order η) the ρ_{13}, ρ_{31}, ρ_{23}, and ρ_{32} terms in Eqs. 1(a) through 1(c), yielding differential equations that include all corrections up

to first order in η [1]:

$$\dot{\rho}_{11} = \left(\frac{i\Omega_2(t)}{2} + \frac{\gamma\Omega_2(t)}{4\omega_{23}}\right)\rho_{12} - \left(\frac{i\Omega_2^*(t)}{2} - \frac{\gamma\Omega_2^*(t)}{4\omega_{23}}\right)\rho_{21} + \frac{\gamma}{2}\rho_{22},$$
$$\dot{\rho}_{12} = \frac{i\Omega_2^*(t)}{2}\rho_{11} - \left(\frac{\gamma}{2} + i\Delta_2'(t)\right)\rho_{12} - \frac{i\Omega_2^*}{2}\rho_{22},$$
$$\dot{\rho}_{22} = \frac{i\Omega_2^*(t)}{2}\rho_{21} - \frac{i\Omega_2(t)}{2}\rho_{12} - \gamma\rho_{22}, \quad (3)$$

where

$$\Delta_2'(t) = \Delta_2 + \frac{|\Omega_3(t)|^2}{4\omega_{23}}. \quad (4)$$

The difference between Δ_2' and Δ_2 leads to a shift in the resonance, but this shift is just the usual ac Stark shift for the interval, and is too small to be of concern for the intensities I_0 considered here. Equation (3) is valid for both σ_+ and σ_-, with the sign differences from $\Omega_3 = \pm\Omega_2$ and from $\gamma_{23\to1} = \pm\gamma/2$ having canceled out. The $\omega_{23}{}^{-1}$ terms result from the nonzero value of $\gamma_{23\to1}$, and these interference terms lead to a shift in the resonance line center, which, unlike the ac Stark shift, does not extrapolate to zero as the laser intensity goes to zero.

To obtain the final population in $|0\rangle$, one can numerically integrate Eq. (3) from t_i to t_f. Since all of the population has radiatively decayed to either $|0\rangle$ or $|1\rangle$ by time t_f, the detection signal $\rho_{00}(t_f)$ is given by $1 - \rho_{11}(t_f)$. The numerical integration is repeated for a set of laser frequencies near the resonance, leading to a calculated resonance line shape, an example of which is shown in Fig. 3(a). The difference between this line shape and the line shape that would result if $\gamma_{23\to1} = 0$ is shown in Fig. 3(c). This difference is due to quantum-mechanical interference with the distant $|1\rangle \to |3\rangle$ resonance and, because it is not symmetric about the line center, it results in a shift in the observed resonance.

A similar derivation can be made for frequencies $\omega = 2\pi f$ that are nearly in resonance with the $|1\rangle \to |3\rangle$ transition, leading to a set of equations similar to Eq. (3), but with $|2\rangle$ and $|3\rangle$ interchanged. Since $\omega_{32} = -\omega_{23}$ and $|\Omega_2|^2 = |\Omega_3|^2$, the interference shifts for the $|1\rangle \to |2\rangle$ and $|1\rangle \to |3\rangle$ resonances are equal in magnitude and opposite in sign, as can be seen in Fig. 3(d). The effect on the deduced $2\,^3P_1$-to-$2\,^3P_2$ interval is therefore twice the shift for each of the laser transitions.

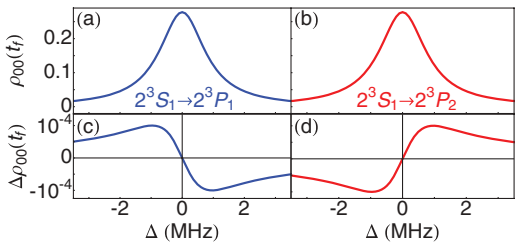

FIG. 3. (Color online) Line shapes of the $|1\rangle \to |2\rangle$ (a) and $|1\rangle \to |3\rangle$ (b) resonances of Fig. 1 obtained from numerical integration of Eq. (3) for the laser beam of Fig. 2 with $T_L = 4$ μs and $I_0 = 10$ μW/cm^2. The differences, (c) and (d), between these line shapes and those that would result if $\gamma_{23\to1} = 0$ are due to the interference effects calculated in this work.

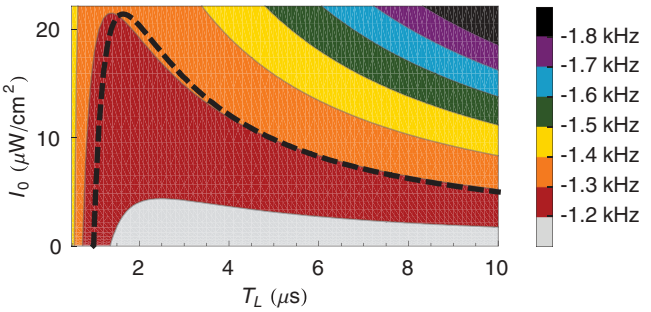

FIG. 4. (Color online) Contour plot of the shift (in kHz) for the $2\,^3P_1$-to-$2\,^3P_2$ interval. The shift is in addition to a small ac shift of Eq. (4) and results from quantum-mechanical interference. The region below the dashed line has a FWHM of the resonance <1.8 MHz.

The shifts of the resonances can be obtained from the numerical calculation of the signal $S(f)$ using

$$\text{shift} = \frac{1}{2}[S(\Delta f) - S(-\Delta f)] \Big/ \left|\frac{dS}{df}\right|_{\Delta f}, \quad (5)$$

where $\pm\Delta f$ are symmetric points around the line center that are near half maximum. Our calculated shifts depend on I_0 and T_L of Fig. 2, and a contour plot of the shifts versus these two variables is shown in Fig. 4. Also shown on this plot is the region of interest for precision measurements in which the full width at half maximum (FWHM) of the laser resonances is less than 1.8 MHz (1.1 times the 1.63 MHz natural width). The measurement of Ref. [15] occurs within this region, as can be seen from the linewidth shown in that work. Note that the shift within this region is approximately constant.

In Ref. [15], the line center was determined using Eq. (5), with most of the data taken at two symmetric half maximum points. Some data was taken at other choices of Δf (that is, at two symmetric points that are not at half maximum), and since the quantum-mechanical interference causes an effect that depends on frequency [Figs. 3(c) and 3(d)], the shift observed [Eq. (5)] will depend on the choice of Δf. The measured values of the fine-structure interval as a function of Δf are shown in Fig. 5(a). After each data point is corrected for the interference effect calculated here, the intervals determined using different Δf become consistent with each other. Of note is the point at $\Delta f = 1.5$ MHz, which had a 3.2σ discrepancy without the interference correction, which is larger at this Δf due to the small dS/df of Eq. (5). The final corrected value for the interval [dashed line of Fig. 5(a)] is 2 291 177.1 ± 1.0 kHz, which includes an average correction of 1.2 ± 0.1 kHz (cf. Fig. 4).

Figure 5(b) compares this corrected value to other experiments and theory. The other laser measurement of this interval [17] may also be subject to an interference effect, but that experiment uses a more complicated saturated absorption technique, which involves two laser beams in an rf discharge cell, and which also involves a substantial magnetic field. The analysis of the interference shift for that experiment is beyond the scope of the present work. The most accurate determination of the interval comes from a microwave separated-oscillatory-field measurement [4]. That measurement has smaller

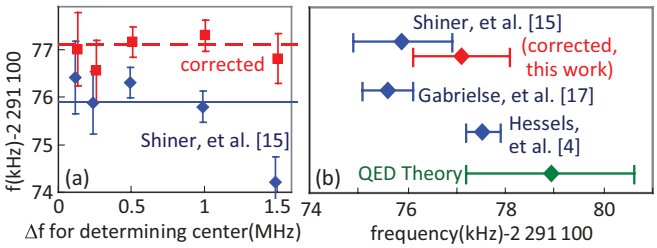

FIG. 5. (Color online) (a) Fine-structure interval inferred from signals at $\pm\Delta f$. The diamonds and uncertainties are from Ref. [15], and the solid line is the final result presented in that work. The squares are corrected for interference shifts calculated in this work. (b) A comparison of measurements and theory for the $2\,^3P_1$-to-$2\,^3P_2$ interval. The measurement of Ref. [15] is shown along with the corrected result from this work. The measurement of Ref. [17] may also be subject to interference corrections, but that calculation is beyond the scope of this work. The microwave measurement of Ref. [4] has only a small interference correction [2]. The QED theory [12] is also shown.

interference shifts (less than 10% of its uncertainty [2]) because the nearest-neighboring resonance is 27.3 GHz away (compared to 2.3 GHz for the resonances studied here) and because the Ramsey method of separated oscillatory fields leads to reduced interference shifts. The corrected value of Ref. [15] and the microwave measurement [4] are in good agreement with each other and with the precise QED calculations of Ref. [12].

In summary, we have calculated corrections due to quantum mechanical interference from distant neighboring resonances for laser transitions for the $2\,^3S$-to-$2\,^3P$ transitions of atomic helium. The calculated corrections are larger than the experimental uncertainties for the measurements, and their inclusion is a necessary step towards the program of obtaining a part-per-billion determination of α from helium $2\,^3P$ fine structure.

Similar interference shifts can also be expected to be significant for laser transitions in other precision measurements, and calculations similar to those presented here should be applied to these other measurements to ensure that this systematic correction is properly applied.

This work is supported by NSERC, CRC, ORF, CFI, and NIST, with computations done using SHARCNET.

[1] M. Horbatsch and E. A. Hessels, Phys. Rev. A **82**, 052519 (2010); **84**, 032508 (2011).

[2] A. Marsman, M. Horbatsch, and E. A. Hessels, Phys. Rev. A **86**, 012510 (2012).

[3] M. C. George, L. D. Lombardi, and E. A. Hessels, Phys. Rev. Lett. **87**, 173002 (2001).

[4] J. S. Borbely, M. C. George, L. D. Lombardi, M. Weel, D. W. Fitzakerley, and E. A. Hessels, Phys. Rev. A **79**, 060503 (2009).

[5] C. Schwartz, Phys. Rev. **134**, A1181 (1964).

[6] B. Schiff, C. L. Pekeris, and H. Lifson, Phys. Rev. **137**, A1672 (1965).

[7] L. Hambro, Phys. Rev. A **7**, 479 (1973); M. Douglas and N. M. Kroll, Ann. Phys. (NY) **82**, 89 (1974); J. Daley, M. Douglas, L. Hambro, and N. M. Kroll, Phys. Rev. Lett. **29**, 12 (1972).

[8] M. L. Lewis and P. H. Serafino, Phys. Rev. A **18**, 867 (1978).

[9] Z.-C. Yan and G. W. F. Drake, Phys. Rev. Lett. **74**, 4791 (1995); T. Zhang, Z.-C. Yan, and G. W. F. Drake, *ibid.* **77**, 1715 (1996); G. W. F. Drake, Can. J. Phys. **80**, 1195 (2002).

[10] K. Pachucki and J. Sapirstein, J. Phys. B **33**, 5297 (2000); **36**, 803 (2003).

[11] K. Pachucki, Phys. Rev. Lett. **97**, 013002 (2006).

[12] K. Pachucki and V. A. Yerokhin, Phys. Rev. Lett. **104**, 070403 (2010).

[13] F. M. J. Pichanick, R. D. Swift, C. E. Johnson, and V. W. Hughes, Phys. Rev. **169**, 55 (1968); A. Kponou, V. W. Hughes, C. E. Johnson, S. A. Lewis, and F. M. J. Pichanick, Phys. Rev. Lett. **26**, 1613 (1971); Phys. Rev. A **24**, 264 (1981); W. Frieze, E. A. Hinds, V. W. Hughes, and F. M. J. Pichanick, *ibid.* **24**, 279 (1981).

[14] D. Shiner, R. Dixson, and P. Zhao, Phys. Rev. Lett. **72**, 1802 (1994); D. L. Shiner and R. Dixson, IEEE Trans. Instr. Meas. **44**, 518 (1995); M. Smiciklas and D. Shiner, Phys. Rev. Lett. **105**, 123001 (2010).

[15] J. Castillega, D. Livingston, A. Sanders, and D. Shiner, Phys. Rev. Lett. **84**, 4321 (2000).

[16] F. Minardi, G. Bianchini, P. C. Pastor, G. Giusfredi, F. S. Pavone, and M. Inguscio, Phys. Rev. Lett. **82**, 1112 (1999); P. C. Pastor, G. Giusfredi, P. De Natale, G. Hagel, C. de Mauro, and M. Inguscio, *ibid.* **92**, 023001 (2004); G. Giusfredi *et al.*, Can. J. Phys. **83**, 301 (2005).

[17] T. Zelevinsky, D. Farkas, and G. Gabrielse, Phys. Rev. Lett. **95**, 203001 (2005).

[18] C. H. Storry and E. A. Hessels, Phys. Rev. A **58**, R8 (1998); C. H. Storry, M. C. George, and E. A. Hessels, Phys. Rev. Lett. **84**, 3274 (2000).

[19] D. A. Cardimona, M. G. Raymer, and C. R. Stroud, Jr., J. Phys. B **15**, 55 (1982); D. A. Cardimona and C. R. Stroud, Jr., Phys. Rev. A **27**, 2456 (1983).